Electronic supplementary information (ESI)

Bifunctional Nanoparticles for SERS Monitoring and Magnetic Intervention of Assembly and Enzyme Cutting of DNAs

Liqin Lin,[a,b] Elizabeth Crew,[a] Hong Yan,[a] Shiyao Shan,[a] Zakiya Skeete,[a] Derrick Mott,[c] Tatiana Krentsel,[a] Jun Yin,[a] Natasha A. Chemova,[a] Jin Luo,[a] Mark H. Engelhard,[d] Chongmin Wang,[d] Qingbiao Li[b], and Chuan-Jian Zhong*[a]

[a] Department of Chemistry, State University of New York at Binghamton, Binghamton, New York 13902, USA

[b] Environmental Science Research Center, College of Environment and Ecology, Xiamen University, Xiamen 361005, China

[c] School of Materials Science, Japan Advanced Institute of Science and Technology, 1-1 Asahidai, Nomi, 923-1292 Ishikawa, Japan

[d] EMSL, Pacific Northwest National Laboratory, Richland, Washington 99352, USA

* To whom correspondence should be addressed. Email: cjzhong@binghamton.edu

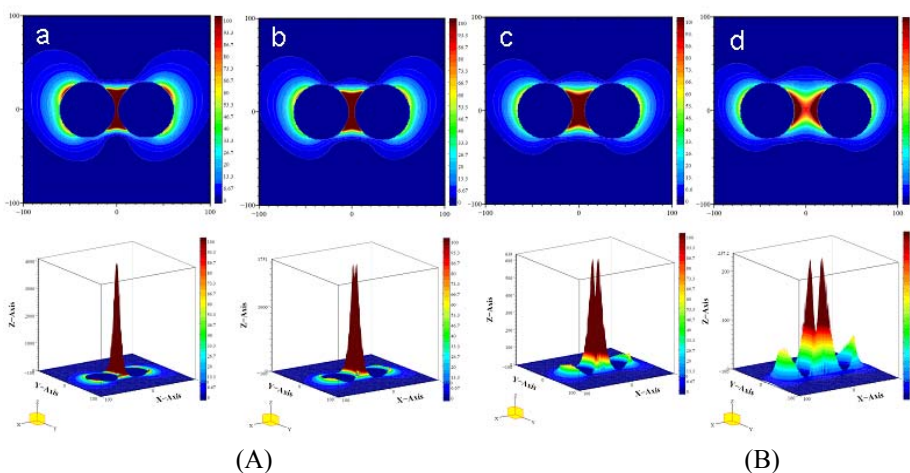**1. Additional Theoretical and Experimental Data**

Figure S1. (A) E-field enhancement contours external to a dimer of Ag nanoparticles (60 nm) with different spacing, for a plane that is along the inter-particle axis and that passes midway throng the two particles. (a) Distance: 3 nm; (b) Distance: 6 nm; (c) Distance: 12 nm; (d) Distance: 24 nm. In the 3D plots, the axis

perpendicular to the selected plane represents the amount of E-field enhancement around the dimer. (a) 548 nm; (b) Right: 518 nm; (c) 490 nm; (d) 465 nm. (We thank Professor S. Zou for his help in providing the calculation result)
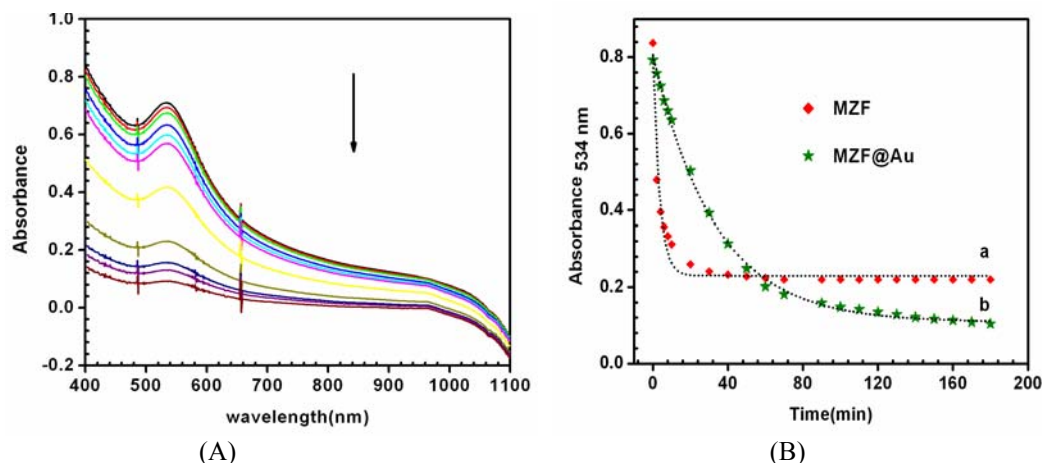

(A)   (B)

Figure S2. Optical and magnetic properties for *MZF/Au* nanoparticles (10.9±2.7 nm; Insert: MZF nanoparticle seeds (8.1±1.5 nm)): (A) UV-vis spectra showing the changes of the SP band vs. time for an aqueous solution of the nanoparticles in a cuvette upon applying a magnet to it, during which the nanoparticles are gradually separated from the solution; (B) Plots showing the magnetic separation kinetics in terms of the change in absorbance (Abs) of the SP band at ∼534 nm for a solution of MZF (a), and *MZF/Au* (b) [Fitting: Abs = 0.230 + 0.576 exp(-0.293*t) (a), Abs = 0.108 + 0.695 exp(-0.031*t) (b)].

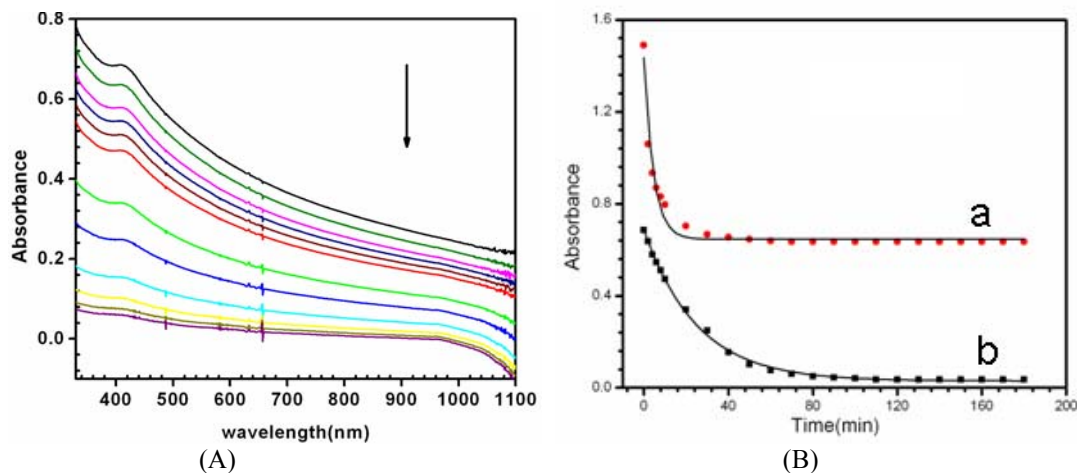(A)   (B)

Figure S3. Optical and magnetic properties for *MZF/Ag* nanoparticles (8.6±1.4 nm; Insert: MZF nanoparticle seeds (8.1±1.5 nm)): (A) UV-vis spectra showing the changes of the SP band vs. time for an aqueous solution of the nanoparticles in a cuvette upon applying a magnet to it, during which the nanoparticles are gradually separated from the solution; (B) Plots showing the magnetic separation kinetics in terms of the change in absorbance (Abs) of the SP band at ∼408 nm for a solution of MZF (a), and *MZF/Ag* (b) [Fitting: Abs = 0.667 + 0.777 exp(-0.242*t) (a), Abs = 0.029 + 0.658 exp(-0.040*t)(b)].

Theoretical consideration of the optical properties: In Figure S2-S3, it is clear that not only the SP band peak's absorbance decreases, but also the absorbance in the entire visible and near region decreases as a function of time upon applying the magnetic field. This observation SP absorption contains contributions in a broad spectral range. To under this observation, we analyzed the shell thickness change

of metal-coated small concentric sphere model based on Mie theory.[1] This model was in fact successfully applied to several different core-shell nanoparticles by Mulvaney[2] and recently utilized by other researchers.[3,4] In the equation for coated small concentric sphere model, the extinction cross section C_{ext} of a small, concentric sphere is given by[5]

$$C_{ext} = 4\pi R^2 k * \times \mathrm{Im}\left[\frac{(\varepsilon_{shell} - \varepsilon_m)(\varepsilon_{core} + 2\varepsilon_{shell}) + (1-g)(\varepsilon_{core} - \varepsilon_{shell})(\varepsilon_m + 2\varepsilon_{shell})}{(\varepsilon_{shell} + 2\varepsilon_m)(\varepsilon_{core} + 2\varepsilon_{shell}) + (1-g)(2\varepsilon_{shell} - 2\varepsilon_m)(\varepsilon_{core} - \varepsilon_{shell})}\right] \quad (1)$$

where ε_{core} is the complex dielectric function of the core material, ε_{shell} is for the shell, ε_m is the real dielectric function of the surrounding medium, g is the volume fraction of the shell layer, and R is the radius of the coated particle. The volume fraction (g) is expressed as:

$$g = 1 - \left(1 - \frac{d_{shell}}{R}\right)^3 \quad (2)$$

where d_{shell} is the thickness of shell, from which the relative core-shell thicknesses can be derived.

Based on the models, we obtained simulation results for core-shell nanoparticles consisting of Fe_3O_4@Au and Fe_3O_4@Ag (Figure S4)[6] (We used Fe_3O_4 core, in MnZnFerrite core, for the simulation because the optical parameters are not readily available at this time). The wavelength of the SP band can be tuned by varying the shell thickness based on calculation results, depending on the core-shell combination. The result that the SP band shifts from visible to near infrared region as shell thickness decreases is consistent with the observation that the experimental spectra spanned to near IR region, suggesting that the *MZF/Au or Ag* nanoparticles likely have various shell thickness.
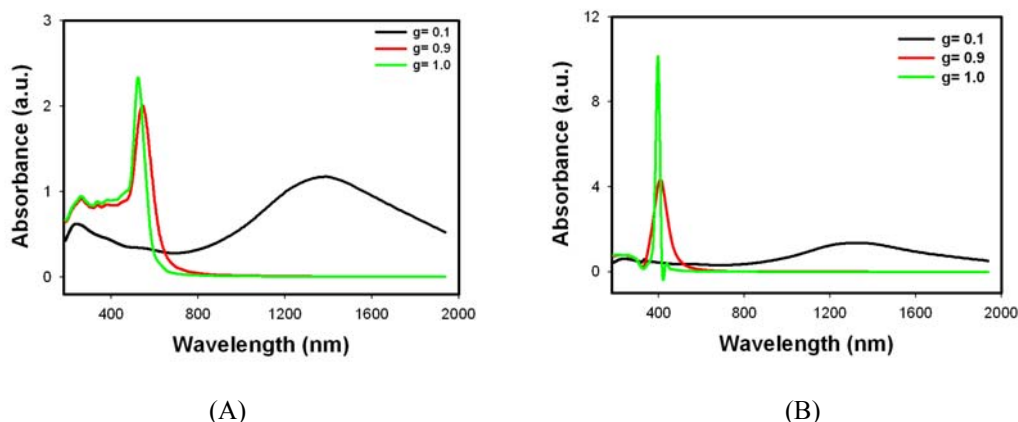

(A) (B)

Figure S4. Simulation results for core-shell nanoparticles consisting of (A) Fe_3O_4@Au (g=1: Au only) and (B) Fe_3O_4@Ag (g=1: Ag only). $\varepsilon_m = 2$.
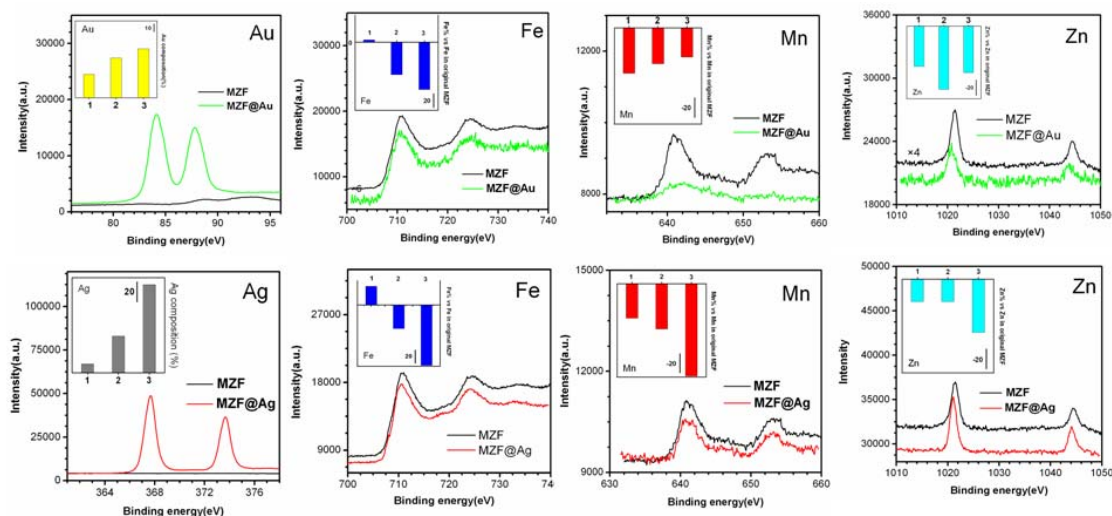
3

Figure S5. XPS analysis results of MZF/Au and MZF/Ag nanoparticles. (Upper panel): Data in the Au 4f, Fe 2p, Zn 2p and Mn 2p regions for samples of MZF/Au. (Bottom panel): Data in the Ag 3d, Fe 2p, Zn 2p and Mn 2p regions for samples of MZF/Ag (The data for the actual MZF particles are included for comparison); Bar charts in the inset showing the relative changes of the Fe, Zn, and Mn compositions (in atomic %) with the increase of Au or Ag coating thickness for MZF/Au and MZF/Ag, with respect to the corresponding MZF nanoparticles.

Table S1. Comparison of binding energy values for *MZF/Au* or *MZF/Ag* nanoparticles before and after coating Au or Ag

Sample	Composition	Binding energy (eV)						
	Au% or (Ag%)	Fe 2p$_{3/2}$		Zn 2p$_{3/2}$		Mn 2p$_{3/2}$		Au 4f$_{7/2}$ or (Ag 3d$_{5/2}$)
		before	after	before	after	before	after	
MZF/Au	63.7	710.93	710.57	1021.38	1020.81	641.13	642.06	84.12
MZF/Ag	38.8	710.93	710.45	1021.38	1021.06	641.13	641.13	367.67

Note: C1s at 284.80 eV was used as internal calibration. For Au and Ag metals, the binding energy (BE) is 84.00 eV for Au4f$_{7/2}$ and 368.22 eV for Ag3d$_{5/2}$, respectively[6].

Table S2. Enhancement factors (EF) calculated from the SERS data for *ds*-DNA assemblies of nanoparticles of different combinations with MBA-Au NPs (39 nm) in aqueous solutions

ds-DNA Assembly	EF
MBA-Au-DNA1/DNA2-*MZF/Au* (11 nm)	7.1×10^4
MBA-Au-DNA1/DNA2-Au (13 nm)	2.9×10^5
MBA-Au-DNA1/DNA2-*MZF/Ag* (9 nm)	1.5×10^5
MBA-Au-DNA1/DNA2-Ag (4 nm)	2.8×10^5
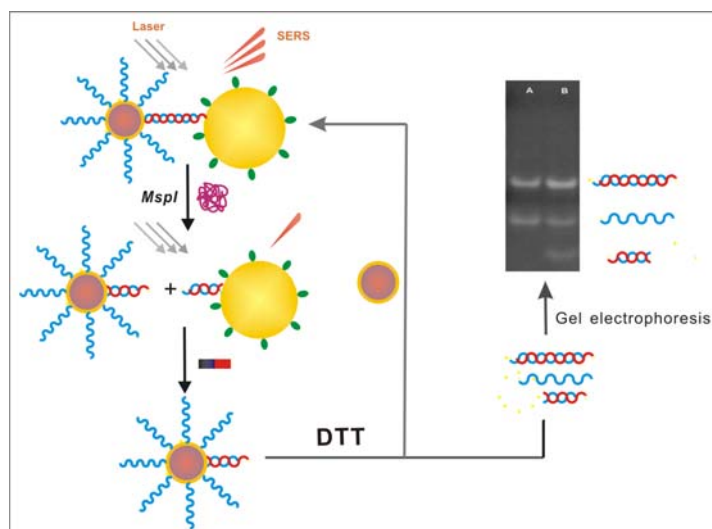
Scheme S1. A schematic diagram illustrates enzymatic cutting of ds-DNAs in the assemblies and magnetic separation of MZF/Au (or MZF/Ag). (DTT: dithiothreitol). Gel electrophoresis data (Lane A: before enzyme cutting; Lane B: after enzyme cutting.)
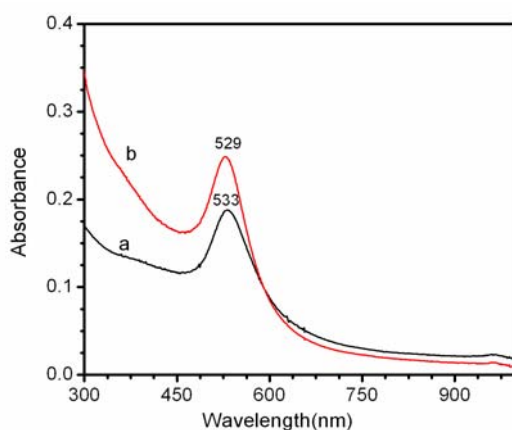

Figure S6. UV-Vis spectra of MBA-Au-DNA1/DNA2-MZF/Au NPs after enzyme cutting and magnetic separation. (a) MZF/Au; (b) Au NPs.
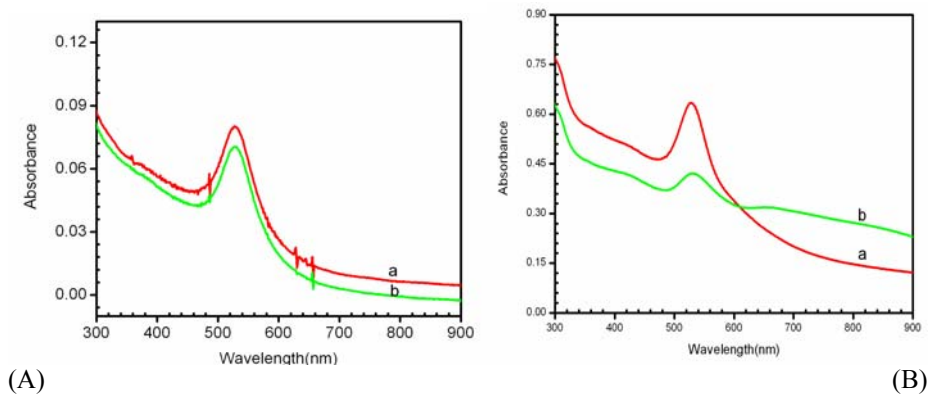

(A)

(B)

Figure S7. UV-vis spectra for an aqueous solution of *MZF/Au*-DNA1 and MBA-Au NPs (A) or *MZF/Ag*-DNA1 and MBA-Au NPs before (a) and after (b) adding DNA2. (A) [*MZF/Au*-DNA1]= 6.2 nM; [DNA2]=0.56 μM; [39 nm Au-MBA]=4.3×10^{-2} nM; (B) [*MZF/Ag*-DNA1]=3.0 nM; [DNA2]=0.56 μM; [39 nm-Au@MBA]= 4.3×10^{-2} nM.
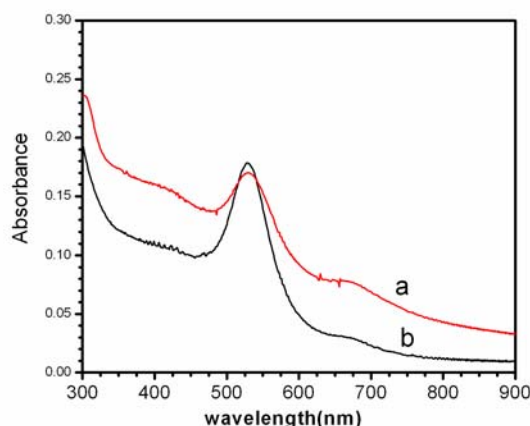

Figure S8. UV-Vis spectra of MBA-Au-DNA1/DNA2-MZF/Ag NPs after enzyme cutting and magnetic separation. (a) MZF/Ag; (b) Au NPs.

Calculation of enhancement factor (EF): EF was estimated based on the following relationship.

$$EF = \frac{I_S / N_S}{I_R / N_R} = \frac{I_S}{I_R} \times \frac{\dfrac{m_{MBA}}{MW_{MBA} \times V} \times N_o}{\dfrac{N_{NPs}}{mL} \times \dfrac{N(MBA)}{NP}} \qquad (3)$$

(I_S: Raman intensity in the DNA assembly sample; I_R: Raman intensity of high concentration of MBA in aqueous solution; m: mass of MBA, MW_{MBA}: molecular weight of MBA; V: the volume of H$_2$O and NaOH using to dissolve MBA; NPs/mL: the number of AuNPs per mL, ligand/NP: the number of MBA per gold nanoparticle.)

References:

1. C. F. Bohren and D. R. Huffman, Absorption and Scattering of Light by Small Particles, Wiley, New York, 1983.
2. P. Mulvaney, *Langmuir*, 1996, **12**, 788.
3. B. M. Reinhard, M. Siu, H. Agarwal, A. P. Alivisatos and J. Liphardt, *Nano Lett.*, 2005, **5**, 2246.
4. D. I. Garcia-Gutierrez, C. E. Gutierrez-Wing, L Giovanetti, J. M. Ramallo-Lopez, F. G. Requejo and M. Jose-Yacaman, *J. Phys. Chem. B*, 2005, **109**, 3813.
5. P. Mulvaney, *Langmuir*, 1996, **12**, 788.
6. J. Luo, L.Y. Wang, D. Mott, P. Njoki, Y. Lin, T. He, Z. Xu, B. Wanjana, I-I. S. Lim, C. J. Zhong, *Adv. Mater.*, 2008, **20**, 4342.
7. H. Yan, I-I. S. Lim, L. C. Zhang, S. C. Gao, D. Mott, Y. Le, D. L. An, C. J. Zhong, *J. Mater. Chem.* **2011**, *21*, 1890.